Moving Beyond a Peak Mentality: Plateaus, Shoulders, Oscillations and Other 'Anomalous' Behavior-Driven Shapes in COVID-19 Outbreaks

Joshua S. Weitz,[1,2,3,*] Sang Woo Park,[4] Ceyhun Eksin,[5] and Jonathan Dushoff[6,7]

[1] *School of Biological Sciences, Georgia Institute of Technology, Atlanta, GA, USA*
[2] *School of Physics, Georgia Institute of Technology, Atlanta, GA, USA*
[3] *Center for Microbial Dynamics and Infection, Georgia Institute of Technology, Atlanta, GA, USA*
[4] *Department of Ecology and Evolutionary Biology, Princeton University, Princeton, NJ, USA*
[5] *Department of Industrial and Systems Engineering, Texas A&M, College Station, Texas, USA*
[6] *Department of Biology, McMaster University, Hamilton, ON, Canada*
[7] *DeGroote Institute for Infectious Disease Research, McMaster University, Hamilton, ON, Canada*

(Dated: September 6, 2020)

The COVID-19 pandemic has caused more than XXXX reported deaths globally, of which more than YYY have been reported in the United States as of XXXX. Public health interventions have had significant impacts in reducing transmission and in averting even more deaths. Nonetheless, in many jurisdictions the decline of cases and fatalities after apparent epidemic peaks has not been rapid. Instead, the asymmetric decline in cases appears, in most cases, to be consistent with plateau- or shoulder-like phenomena – a qualitative observation reinforced by a symmetry analysis of US state-level fatality data. Here we explore a model of fatality-driven awareness in which individual protective measures increase with death rates. In this model, epidemic dynamics can be characterized by plateaus, shoulders, and lag-driven oscillations after exponential rises at the outset of disease dynamics. We find that model-predicted outcomes are consistent with asymmetric shape of observed peaks. Yet, in contrast to model predictions, we find that population-level estimates of mobility usually increased *before* peak levels of fatalities. We show that incorporating fatigue and and long-term behavior change can reconcile the apparent premature relaxation of mobility reductions and dictate whether post-peak dynamics leads to a resurgence of cases or epidemic declines.

Significance statement:
In contrast to predictions of conventional epidemic models, COVID-19 dynamics have asymmetric shapes, with cases and fatalities declining much more slowly than they rose. This manuscript evaluates how awareness-driven behavior modulates epidemic shape. We find that short-term awareness of fatalities leads to emergent plateaus, persistent shoulder-like dynamics, and lag-driven oscillations in a SEIR-like model; consistent with analysis of US state-level data. However in contrast to model predictions, a joint analysis of fatalities and mobility suggest that populations relaxed mobility restrictions prior to fatality peaks. We show that incorporating fatigue and long-term behavior change dictates post-peak outcomes spanning case resurgence to sustained epidemic declines. These findings suggest the need to incorporate behavior-driven feedback in epidemic models and in public health campaigns to control COVID-19 spread.

I. INTRODUCTION

The spread of COVID-19 has elevated the importance of epidemiological models as a means to forecast both near- and long-term spread. In the United States, the Institute for Health Metrics and Evaluation (IHME) model has emerged as a key influencer of state- and national-level policy [1]. The IHME model includes a detailed characterization of the variation in hospital bed capacity, ICU beds, and ventilators between and within states. Predicting the projected strains on underlying health resources is critical to supporting planning efforts. However such projections require an epidemic 'forecast'. The IHME's epidemic forecast differs from conventional epidemic models in a significant way – IHME assumes that the cumulative deaths in the COVID-19 epidemic follow a symmetric, Gaussian-like trajectory. For example, the IHME model predicts that if the peak is 2 weeks away then in 4 weeks cases will return to the level of the present, and continue to diminish rapidly. But, epidemics need not have one symmetric peak – the archaic Farr's Law of Epidemics notwithstanding (see [2] for a cautionary tale of using Farr's law as applied to the HIV epidemic).

Conventional epidemic models of COVID-19 represent populations in terms of their 'status' vis a vis the infectious agent, i.e., susceptible, exposed, infectious, hospitalized, and recovered [3–9]. New transmission can lead to an exponential increases in cases when the basic reproduction number $\mathcal{R}_0 > 1$ (the basic reproduction number denotes the average number of new infections caused by a single, typical individual in an otherwise susceptible population [10]). Subsequent spread, if left unchecked, would yield a single peak – in theory. That peak corresponds to when 'herd immunity' is reached, such that the effective reproduction number, $\mathcal{R}_{\text{eff}} = 1$. The effective

*Electronic address: jsweitz@gatech.edu; URL: http://ecotheory.biology.gatech.edu

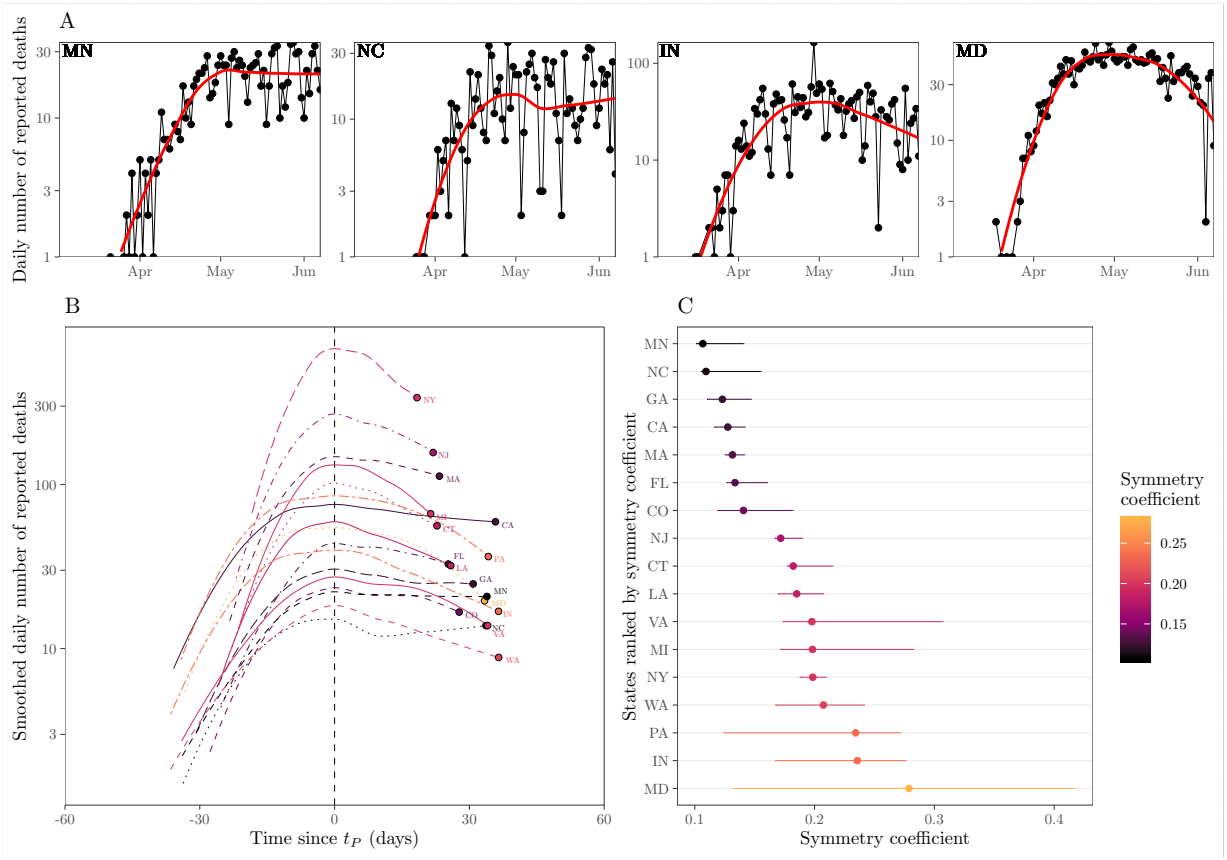

FIG. 1: Plateaus and shoulder-like dynamics in COVID-19 fatalities. (A) Examples of locally estimated scatterplot smoothing (LOESS) of daily number of deaths for COVID-19 in four states, including two estimated to be the most plateau-like (Minnesota and North Carolina) and two estimated to be the most peak-like (Indiana and Maryland). Daily number of deaths is averaged in log space, only including days with one or more reported deaths; US state level averages. (B) Smoothed daily number of reported deaths centered around the first fatality peak of the epidemic for 17 states. (C) Measured symmetry coefficient and confidence intervals. Methods and Supplementary Information contain detailed description of the LOESS smoothing in (A), peak identification in (B), and symmetry coefficient estimator in (C).

reproduction number denotes the number of new infectious cases caused by a single infectious individual in a population with pre-existing circulation. But, even when herd immunity is reached, there will still be new cases which then diminish over time, until the epidemic concludes. A single-peak paradigm is only robust insofar as the disease has spread sufficiently in a population to reach and exceed 'herd immunity'. The converse is also true – as long as a population remains predominantly immunologically naive, then the risk of further infection has not passed.

The Imperial College of London (ICL) model [3] is one of the most influential of epidemiogical models shaping public health responses to COVID-19. The ICL model is an example of a 'conventional' epidemic model that shows the benefits of early intervention steps in reducing transmission and preserving health system resources vs. a 'herd immunity' strategy. The ICL model assumes that transmission is reduced because of externalities, like lockdowns, school closings, and so on. As a result, the ICL model suggests that lifting of large-scale public health interventions could be followed by a second wave of cases. Yet, for a disease that is already the documented cause of more than XXXX deaths in the United States alone, we posit that individuals are likely to continue to modify their behavior even after lockdowns are lifted. Indeed, the peak death rates in the United States and globally are not as high as potential maximums in the event that COVID-19 had spread unhindered in the population [3]. Moreover, rather than a peak and symmetric decline, there is evidence of asymmetric plateaus and shoulder like behavior for daily fatality rates within US-states (Figure 1, full state-level data in Supplementary Figure **??**).

In this manuscript we use a nonlinear model of epidemiological dynamics to ask the question: what is the anticipated shape of an epidemic if individuals modify their behavior in direct response to the impact of a disease at the population level? In doing so, we build upon earlier work on awareness based models (e.g. [11–14])

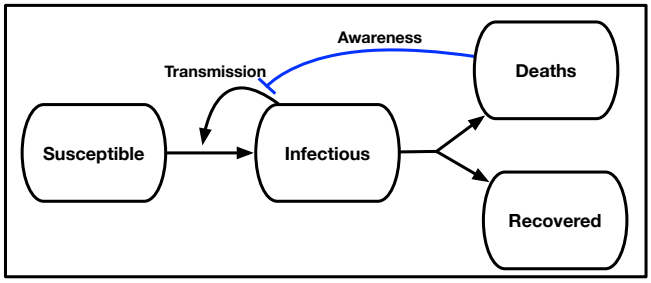

FIG. 2: Schematic of an SEIR model with awareness-driven social distancing. Transmission is reduced based on short- and/or long-term awareness of population-level disease severity (i.e., fatalities).

with an initial assumption: individuals reduce interactions when death rates are high and increase interactions when death rates are low. As we show, short-term awareness can lead to dramatic reductions in death rates compared to models without accounting for behavior, leading to plateaus, shoulders, and lag-driven oscillations in death rates. We also show that dynamics can be driven from persistent dynamics to elimination when awareness shifts from short- to long-term.

II. RESULTS AND DISCUSSION

A. SEIR Model with Short-Term Awareness of Risk

Consider an SEIR like model

$$\dot{S} = -\frac{\beta SI}{\left[1+(\delta/\delta_c)^k\right]} \quad (1)$$

$$\dot{E} = \frac{\beta SI}{\left[1+(\delta/\delta_c)^k\right]} - \mu E \quad (2)$$

$$\dot{I} = \mu E - \gamma I \quad (3)$$

$$\dot{R} = (1-f_D)\gamma I \quad (4)$$

$$\dot{D} = f_D \gamma I \quad (5)$$

where S, E, I, R, and D denote the proportions of susceptible, exposed, infectious, recovered, and deaths, respectively, given transmission rate β /day, transition to infectious rate μ /day, recovery rate γ /day, where f_D is the infection fatality probability. The awareness-based distancing is controlled by the death rate $\delta \equiv \dot{D}$, the half-saturation constant ($\delta_c > 0$), and the sharpness of change in the force of infection ($k \geq 1$) (see Figure 2 for a schematic). Since δ is proportional to I, this model is closely related to a recently proposed awareness-based distancing model [14] and to an independently derived feedback SIR model [15]. Note that the present model converges to the conventional SEIR model as $\delta_c \to \infty$.

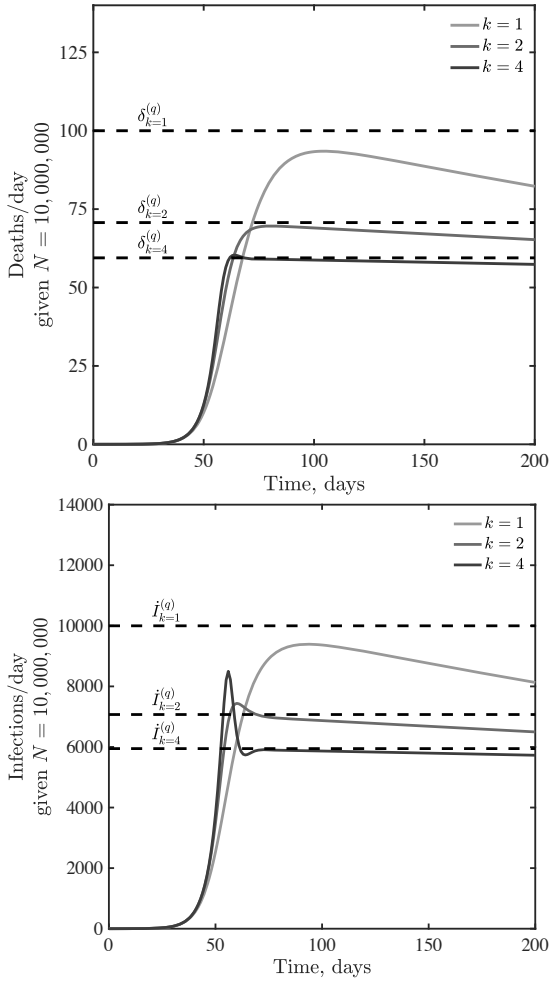

FIG. 3: Infections and deaths per day in a death-awareness based social distancing model. Simulations have the epidemiological parameters $\beta = 0.5$ /day, $\mu = 1/2$ /day, $\gamma = 1/6$/day, and $f_D = 0.01$, with variation in $k = 1$, 2 and 4. We assume $N\delta_c = 50$ /day in all cases.

Uncontrolled epidemics in SEIR models have a single case peak, corresponding to the point where $\gamma I = \beta SI$ such that the population obtains herd immunity when only a proportion $S = 1/\mathcal{R}_0$ have yet to be infected. However, when individuals decrease transmission in relationship to awareness of the population impacts of the disease, $\delta(t)$, then the system can 'peak' when levels of infected cases are far from herd immunity, specifically when

$$\gamma I = \frac{\beta SI}{\left[1+(\delta/\delta_c)^k\right]}. \quad (6)$$

When δ_c is small compared to the per-capita death rate of infectious individuals (γf_D) we anticipate that individual behavior will respond quickly to the disease outbreak. Hence, we hypothesize that the emergence of an awareness-based peak can occur early, i.e., $S(t) \approx 1$,

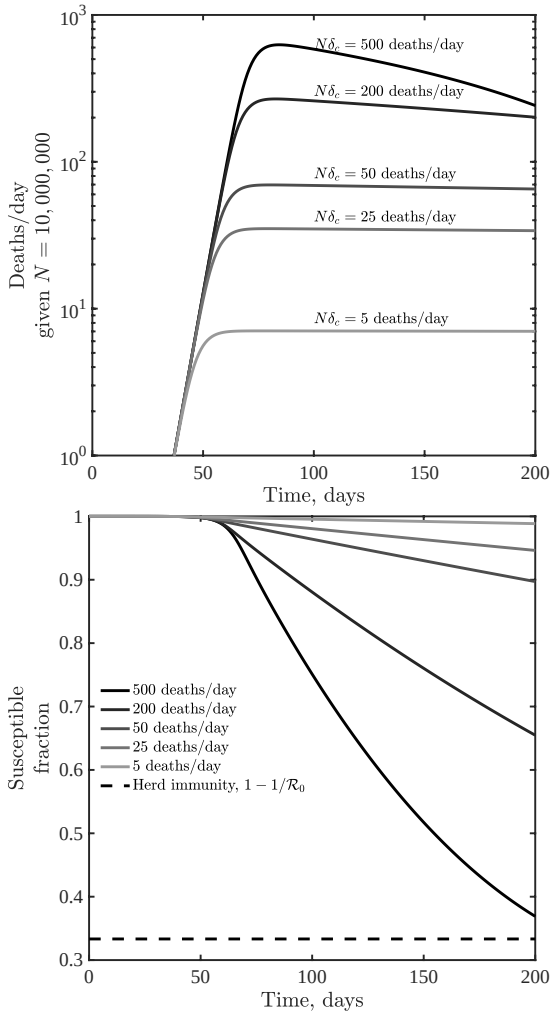

FIG. 4: Dynamics given variation in the critical fatality awareness level, δ_c for awareness $k = 2$. Panels show deaths/day (top) and the susceptible fraction as a function of time (bottom), the latter compared to a herd immunity level when only a fraction $1/\mathcal{R}_0$ remain susceptible. These simulations share the epidemiological parameters $\beta = 0.5$ /day, $\mu = 1/2$ /day, $\gamma = 1/6$ /day, and $f_D = 0.01$.

consistent with a quasi-stationary equilibrium when the death rate is

$$\delta^{(q)} \approx \delta_c \left(\mathcal{R}_0 - 1\right)^{1/k} \tag{7}$$

and the infection rate is

$$\dot{I}^{(q)} \approx \frac{\delta_c}{f_D} \left(\mathcal{R}_0 - 1\right)^{1/k}. \tag{8}$$

These early onset peak rates should arise not because of herd immunity but because of changes in behavior.

We evaluate this hypothesis in Figure 3 for $k = 1$, $k = 2$, and $k = 4$ given disease dynamics with $\beta = 0.5$ /day, $\mu = 1/2$ /day, $\gamma = 1/6$ /day, $f_D = 0.01$, $N = 10^7$, and $N\delta_c = 50$ /day. As is evident, the rise and decline from peaks are not symmetric. Instead, incorporating awareness leads to dynamics where incidence decreases very slowly after a peak. The peaks occur at levels of infection far from that associated with herd immunity. Post-peak, shoulders and plateaus emerge because of the balance between relaxation of awareness-based distancing (which leads to increases in cases and deaths) and an increase in awareness in response to increases in cases and deaths. We note that as k increases, individuals become less sensitive to fatality rates where $\delta < \delta_c$ and more sensitive to fatality rates where $\delta > \delta_c$. This leads to sharper dynamics. In addition, infections can over-shoot the expected plateau given that awareness is driven by fatalities which are offset with respect to new infections.

B. Short-term awareness, long-term plateaus, and oscillations

Initial analysis of an SEIR model with short-term awareness of population-level severity suggests a generic outcome: fatalities will increases exponentially before plateauing near to a level δ_c. Figure 4 shows the results of dynamics given δ_c values over a range equivalent to 5 to 500 deaths/day given a population of 10^7 for $k = 2$ (we note that results for $k = 1$ and $k = 4$ lead to similar findings, see Figure S1). When δ_c is small (compared to (γf_D), fatalities can be sustained at near-constant levels for a long time. When δ_c is higher then the decline of cases and fatalities due to susceptible depletion is relatively fast. Hence, even given significant variation in the critical daily fatality rates, the population remains largely susceptible even as sustained fatalities continue for a period far greater than the time it took to reach the plateau.

To explore the impacts of lags on dynamics, we incorporated an additional class H, assuming that fatalities follow potentially prolonged hospital stays. We do not include detailed information on symptomatic transmission, asymptomatic transmission, hospitalization outcome, age structure, and age-dependent risk (as in [3]). Instead, we consider the extended SEIR model:

$$\dot{S} = -\frac{\beta S I}{\left[1 + \left(\delta/\delta_c\right)^k\right]} \tag{9}$$

$$\dot{E} = \frac{\beta S I}{\left[1 + \left(\delta/\delta_c\right)^k\right]} - \mu E \tag{10}$$

$$\dot{I} = \mu E - \gamma I \tag{11}$$

$$\dot{R} = (1 - f_D)\gamma I \tag{12}$$

$$\dot{H} = f_D \gamma I - \gamma_H H \tag{13}$$

$$\dot{D} = \gamma_H H \tag{14}$$

where $T_H = 1/\gamma_H$ defines the average time in a hospital stay before a fatality. Note, we recognize that many individuals recover from COVID-19 after hospitalization; this model's hospital compartment functions as a prefilter.

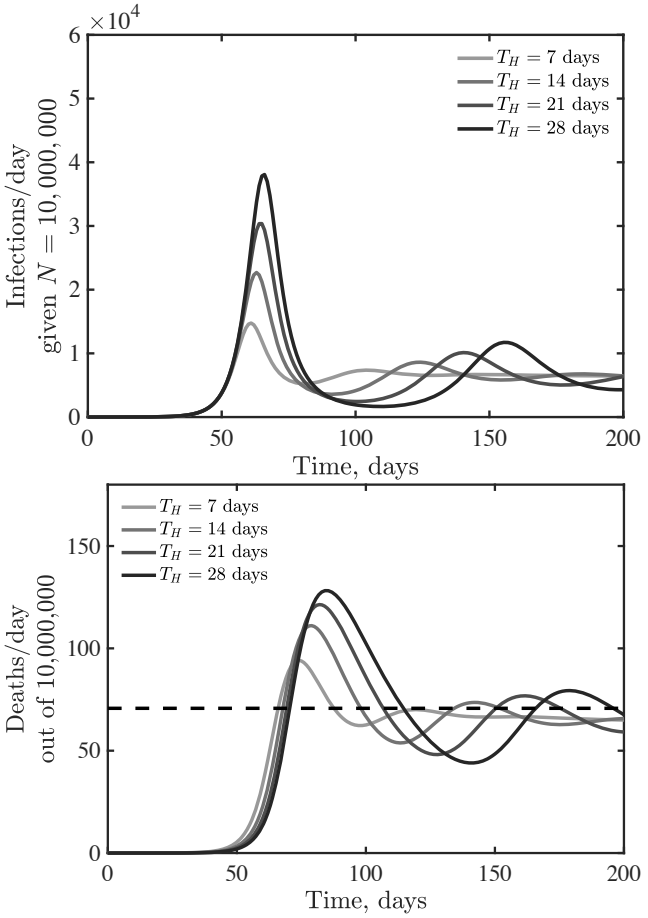

FIG. 5: Emergence of oscillatory dynamics in a death-driven awareness model of social distancing given lags between infection and fatality. Awareness is $k = 2$ and all other parameters as in Figure 3. The dashed lines for fatalities expected quasi-stationary value $\delta^{(q)}$.

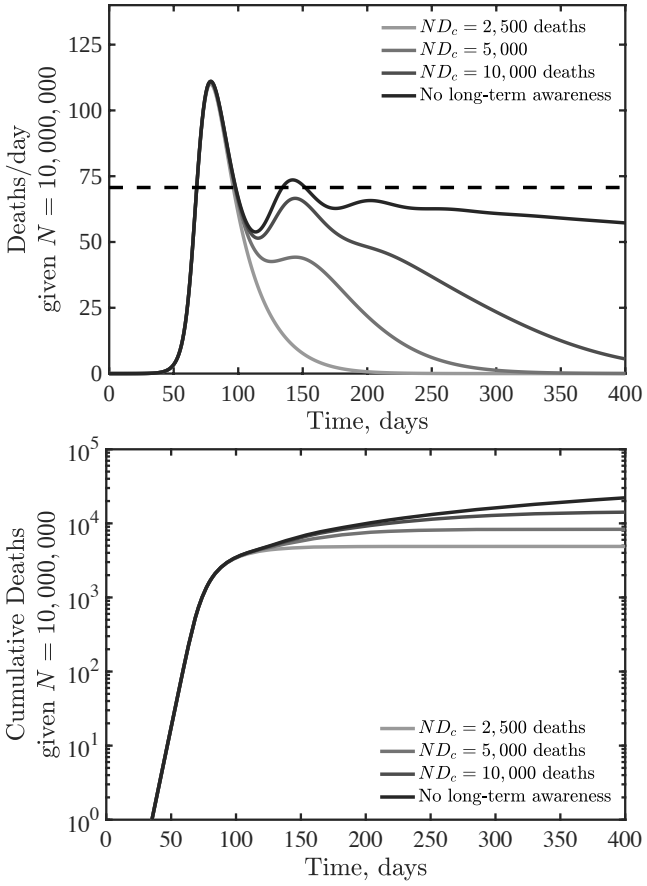

FIG. 6: SEIR dynamics with short- and long-term awareness. Model parameters are $\beta = 0.5$ /day, $\mu = 1/2$ /day, $\gamma = 1/6$ /day, $T_H = 14$ days, $f_D = 0.01$, $N = 10^7$, $k = 2$, $N\delta_c = 50$ /day (short-term awareness), with varying ND_c (long-term awareness) as shown in the legend. The dashed line (top) denotes $\delta^{(q)}$ due to short-term distancing alone.

The earlier analysis of the quasi-stationary equilibrium in fatalities holds in the case of a SEIR model with additional classes before fatalities. Hence, we anticipate that dynamics should converge to $\delta = \delta^{(q)}$ at early times. However, increased delays between cases and fatalities could lead to oscillations in both. Indeed, this is what we find via examination of models in which T_H ranges from 7 to 35 days, with increasing magnitude of oscillations as T_H increases (see Figure 5 for $k = 2$ with qualitatively similar results for $k = 1$ and $k = 4$ shown in Figure S2).

C. Dynamical consequences of short-term and long-term awareness

Awareness can vary in duration, e.g., awareness of SARS-1 may prepare individuals to more readily adopt and retain social distancing measures [16, 17]. In previous work, long-term awareness of cumulative incidence was shown to lead to substantial decreases in final size of epidemics compared to baseline expectations from inferred strength [14]. Hence, we consider an extension of the SEIR model with lags between infection and fatalities that incorporates both short-term and long-term awareness:

$$\dot{S} = -\frac{\beta SI}{\left[1 + (\delta/\delta_c)^k + (D/D_c)^k\right]} \quad (15)$$

$$\dot{E} = \frac{\beta SI}{\left[1 + (\delta/\delta_c)^k + (D/D_c)^k\right]} - \mu E \quad (16)$$

$$\dot{I} = \mu E - \gamma I \quad (17)$$

$$\dot{R} = (1 - f_D)\gamma I \quad (18)$$

$$\dot{H} = f_D \gamma I - \gamma_H H \quad (19)$$

$$\dot{D} = \gamma_H H \quad (20)$$

where D_c denotes a critical cumulative fatality level (and formally a half-saturation constant for the impact of long-term awareness on distancing). Note that the relative

importance of short- and long-term awareness can be modulated by δ_c and D_c respectively. Figure 6 shows daily fatalities (top) and cumulative fatalities (bottom) for an SEIR model with $\mathcal{R}_0 = 2.5$, $T_H = 14$ days, and $N\delta_c = 50$ fatalities per day and critical cumulative fatalities of $ND_c = 2,500$, 5,000, 10,000 as well as a comparison case with vanishing long-term awareness. As is evident, long-term awareness drives dynamics towards rapid declines after reaching a peak. This decline arises because D monotonically increases; increasing fatalities beyond D_c leads to rapid suppression of transmission. However, when δ_c rather than D_c drives dynamics, then shoulders and plateaus can re-emerge. In reality, we expect that individual behavior is shaped by short- and long-term awareness of risks, including the potential for fatigue and 'decay' of long-term behavior change [11, 12].

D. Empirical assessment of mechanistic drivers of asymmetric peaks in Covid-19 death rates

Epidemic models with behavior suggest that awareness-driven distancing underlies the degree of asymmetry surrounding peaks in fatalities. To test this mechanistic link, we jointly analzed the dynamics of fatality rates and behavior, using mobility data obtained from **sources X and Y** as a proxy for behavior (see Methods for the aggregation of multiple mobility metrics via a Principal Component Analysis (PCA)). Notably, we find that aggregated rates of mobility typically began to *increase* before the local peak in fatality was reached (Figure 7A). This rebound in mobility rates implies a collective response akin to opening up too early. For example, in the case of North Carolina, mobility increased even as fatality rates were increasing. Whereas, the state of New York exhibited reversible dynamics in the phase plane, implying that decreases in mobility were tightly linked to fatality rates. As shown in Figure 7B, the shape of dynamics are expected to be 'reversible' (given short-term awareness, analogous to the dynamics in New York) or 'counter-clockwise' (given long-term awareness that would lead to sustained declines in fatalities). Counter-clockwise shapes are not observed in any of the data sets we studied.

We hypothesize that a combination of awareness-driven distancing and fatigue can lead to clockwise like dynamics; implying that changes in behavior are not necessarily monotonically related to near-term or long-term fatalities. Consider the following model of awareness-driven distancing including fatigue:

$$\dot{S} = -\frac{\beta SI}{g(D)} \tag{21}$$

$$\dot{E} = \frac{\beta SI}{g(D)} - \mu E \tag{22}$$

$$\dot{I} = \mu E - \gamma I \tag{23}$$

$$\dot{R} = (1 - f_D)\gamma I \tag{24}$$

$$\dot{H} = f_D \gamma I - \gamma_H H \tag{25}$$

$$\dot{D} = \gamma_H H \tag{26}$$

$$\dot{\beta} = \frac{\epsilon}{2}\left[\frac{\left(\frac{\hat{\beta}}{1+(\delta/\delta_c)^k} - \beta\right)}{1 + (D/D_c)^k} + \left(\hat{\beta} - \beta\right)\right] \tag{27}$$

Here the force of infection is related to the mobility denoted by $\beta(t)$ (which dictates the number of interactions per unit time) modulated by a reduction in risk per infection $g(D)$. In this model, $\hat{\beta}$ denotes the baseline behavior, and ϵ denotes a time-scale for behavior change. The level of fatigue is controlled by D_c, such that mobility returns to a baseline $\hat{\beta}$ once $D \gg D_c$. We consider two models, corresponding to $g(D) = 1$ such that the force of infection depends on mobility alone, and $g(D) = \left(1 + (D/D_c)^k\right)$ corresponding to sustained changes in the risk of infection per contact (e.g., due to mask wearing, contact-less interactions, use of PPE, etc.). As shown in Figure 7C/D, the dynamics switch from counter-clockwise to clockwise in the $\delta - \beta$ plane given the incorporation of fatigue. Deaths drive down mobility, but eventually, decreases in β due to short-term awareness are over-come by fatigue, leading to increases in β. If $g(D) = 1$, then the dynamics include increases in both mobility and fatalities akin to levels expected in the absence of behavior, and eventually levels of infection that are stopped by herd immunity, rather than by awareness (see Figure 7C). In contrast, if there is sustained behavior change such that $g(D)$ decreases with increasing cumulative deaths then there is a single peak that forms a clockwise loop; with the peak close to, but after the minimum in behavior (Figure 7D); as observed in nearly all state-level data sets.

III. CONCLUSIONS

We have developed and analyzed a series of models that assume awareness of disease-induced death can reduce transmission and shown that such awareness-driven feedback can lead to highly asymmetric epidemic curves. Asymmetric curves exhibit extended periods of near-constant cases even as the majority of the population remains susceptible. Hence: passing a 'peak' need not imply the rapid decline of risk. In these conditions, if individuals are unable to sustain social distancing policies, or begin to tolerate higher death rates, then cases could increase (similar results have also been proposed

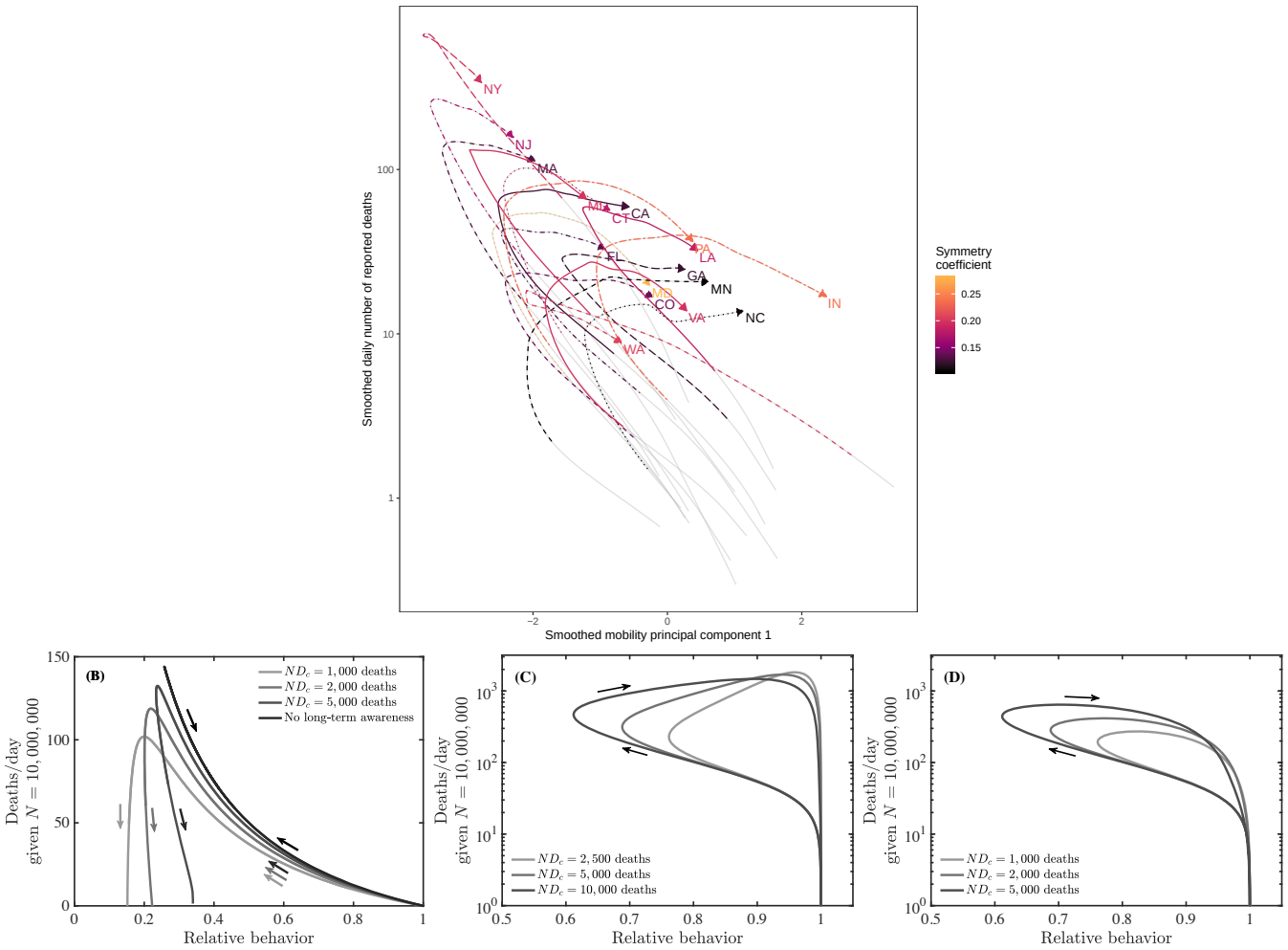

FIG. 7: Dynamics of mobility and fatality for state-level data (top) and SEIR models (bottom panels). (Top) PCA projection of XXXX. FILL IN (B) Dynamics of effective behavior and death rates in a SEIR model with short- and long-term awareness. Curves denote different assumptions regarding long-term awareness, in each case $\beta = 0.5$, $mu = 0.5$, $\gamma = 1/6$, such that $\mathcal{R}_0 = 3$, with $k = 2$, $\gamma_H = 1/21$, and $f_D = 0.01$. The short-term awareness corresponds go $N\delta_c = 50$ deaths/day. Thin lines denote full dynamics over 400 days; thick lines denote the dynamics near the case fatality peak. (C) Dynamics of effective behavior and death rates in a SEIR model with awareness and fatigue. The three different curves denote different assumptions regarding long-term awareness, in each case $\beta = 0.5$, $mu = 0.5$, $\gamma = 1/6$, such that $\mathcal{R}_0 = 3$, with $k = 2$, $\gamma_H = 1/21$, $f_D = 0.01$, and $\epsilon = 1/7$. The short-term awareness corresponds go $N\delta_c = 50$ deaths/day. The force of infection does not include long term changes in behavior beyond mobility, i.e., $g(D) = 1$. (D) As in (C), but the force of infection includes long-term changes in behavior, i.e., $g(D) = 1/\left(1 + (D/D_c)^k\right)$.

in a recent, independently derived feedback SIR model [15]). Indeed, detailed analysis of mobility and fatalities suggest that mobility increased before fatalities peak; consistent with models in which awareness-driven distancing is limited by fatigue. Notably we find that if mobility increases but the risk of infection per interaction decreases due to systemtic changes in behavior, then models suggest 'clockwise' dynamics between behavior and fatality as found in nearly all state-level datasets analyzed here. Awareness-driven endogenous changes in $\mathcal{R}_{\text{eff}}$ are typically absent in models that form the basis for public policy and strategic planning. Our findings highlight the potential impacts of short-term and long-term awareness in efforts to shape information campaigns to reduce transmission after early onset 'peaks', particularly when populations remain predominantly immunologically naive.

Although the models here are intentionally simple, it seems likely that observed asymmetric dynamics of COVID-19, including slow declines and plateau-like behavior, may be an emergent property of awareness-driven epidemiological dynamics. Moving forward, it is essential to fill in significant gaps in understanding how awareness of disease risk and severity shape behavior [18]. Mobility data is a proxy but not equivalent to a direct indicator of transmission risk. Thus far, measurements of

community mobility have been used as a leading indicator for epidemic outcomes. Prior work has shown significant impacts of changes in mobility and behavior on the COVID-19 outbreak [7]. Here we have shown the importance of looking at a complementary feedback mechanism, i.e., from outbreak to behavior. In doing so, we have also shown that decomposing the force of infection in terms of the number of potential transmissions and the probability of infection per contact can lead to outcomes aligned with observed state-level dynamics. Understanding the drivers behind emergent plateaus observed at national and sub-national levels could help decision makers structure intervention efforts appropriately to effectively communicate awareness campaigns that may aid in collective efforts to control the ongoing COVID-19 pandemic.

Data availability: All simulation codes, figures, and data used in the development of this manuscript are available at `https://github.com/jsweitz/covid19-git-plateaus`. Daily number of reported deaths as of May 11, 2020, is obtained from The COVID Tracking Project (covidtracking.com; for US states and territories) and the European Centre for Disease Prevention and Control (https://www.ecdc.europa.eu/en; for 5 countries).

Acknowledgements: Research effort by JSW was enabled by support from grants from the Simons Foundation (SCOPE Award ID 329108), the Army Research Office (W911NF1910384), National Institutes of Health (1R01AI46592-01), and National Science Foundation (1806606 and 1829636). JD was supported in part by grants from the Canadian Institutes of Health Research and the Natural Sciences and Engineering Research Council of Canada.

1 IHME COVID-19 health services utilization forecasting team, Murray CJ (2020) Forecasting COVID-19 impact on hospital bed-days, ICU-days, ventilator-days and deaths by US state in the next 4 months. *medRxiv* `https://www.medrxiv.org/content/10.1101/2020.03.27.20043752v1`.

2 Bregman DJ, Langmuir AD (1990) Farr's law applied to AIDS projections. *JAMA* 263:1522–1525.

3 Ferguson NM, et al. (2020) Impact of non-pharmaceutical interventions (NPIs) to reduce COVID19 mortality and healthcare demand. `https://www.imperial.ac.uk/mrc-global-infectious-disease-analysis/covid-19/report-9-impact-of-npis-on-covid-19/`.

4 Kucharski AJ, et al. (2020) Early dynamics of transmission and control of covid-19: a mathematical modelling study. *The Lancet Infectious Diseases* 20:553 – 558.

5 Kissler SM, Tedijanto C, Goldstein E, Grad YH, Lipsitch M (2020) Projecting the transmission dynamics of SARS-CoV-2 through the post-pandemic period. *Science* p eabb5793.

6 Park SW, et al. (2020) Reconciling early-outbreak estimates of the basic reproductive number and its uncertainty: framework and applications to the novel coronavirus (SARS-CoV-2) outbreak. *medRxiv* `https://www.medrxiv.org/content/10.1101/2020.01.30.20019877v4.full.pdf`.

7 Kraemer MUG, et al. (2020) The effect of human mobility and control measures on the COVID-19 epidemic in china. *Science* 368:493–497.

8 Li R, et al. (2020) Substantial undocumented infection facilitates the rapid dissemination of novel coronavirus (COVID-19). *Science* 368:489–493.

9 Wu J, Leung K, Bushman M, et al. (2020) Estimating clinical severity of COVID-19 from the transmission dynamics in Wuhan, China. *Nature Medicine* 26:506–510.

10 Anderson RM, May RM (1991) *Infectious diseases of humans: dynamics and control* (Oxford university press).

11 Funk S, Gilad E, Watkins C, Jansen VA (2009) The spread of awareness and its impact on epidemic outbreaks. *Proceedings of the National Academy of Sciences* 106:6872–6877.

12 Funk S, Salathé M, Jansen VA (2010) Modelling the influence of human behaviour on the spread of infectious diseases: a review. *Journal of the Royal Society Interface* 7:1247–1256.

13 Eksin C, Shamma JS, Weitz JS (2017) Disease dynamics in a stochastic network game: a little empathy goes a long way in averting outbreaks. *Scientific reports* 7:44122.

14 Eksin C, Paarporn K, Weitz JS (2019) Systematic biases in disease forecasting–The role of behavior change. *Epidemics* 27:96–105.

15 Franco E (2020) A feedback SIR (fSIR) model highlights advantages and limitations of infection-based social distancing. *arXiv preprint arXiv:2004.13216*.

16 Chen H, Xu W, Paris C, Reeson A, Li X (2020) Social distance and SARS memory: impact on the public awareness of 2019 novel coronavirus (COVID-19) outbreak. *medRxiv* `https://www.medrxiv.org/content/10.1101/2020.03.11.20033688v1`.

17 Leung K, Wu JT, Liu D, Leung GM (2020) First-wave COVID-19 transmissibility and severity in China outside Hubei after control measures, and second-wave scenario planning: a modelling impact assessment. *The Lancet* 395:1382 – 1393.

18 West R, Michie S, Rubin GJ, Amlôt R (2020) Applying principles of behaviour change to reduce SARS-CoV-2 transmission. *Nature Human Behaviour* `https://doi.org/10.1038/s41562-020-0887-9`.

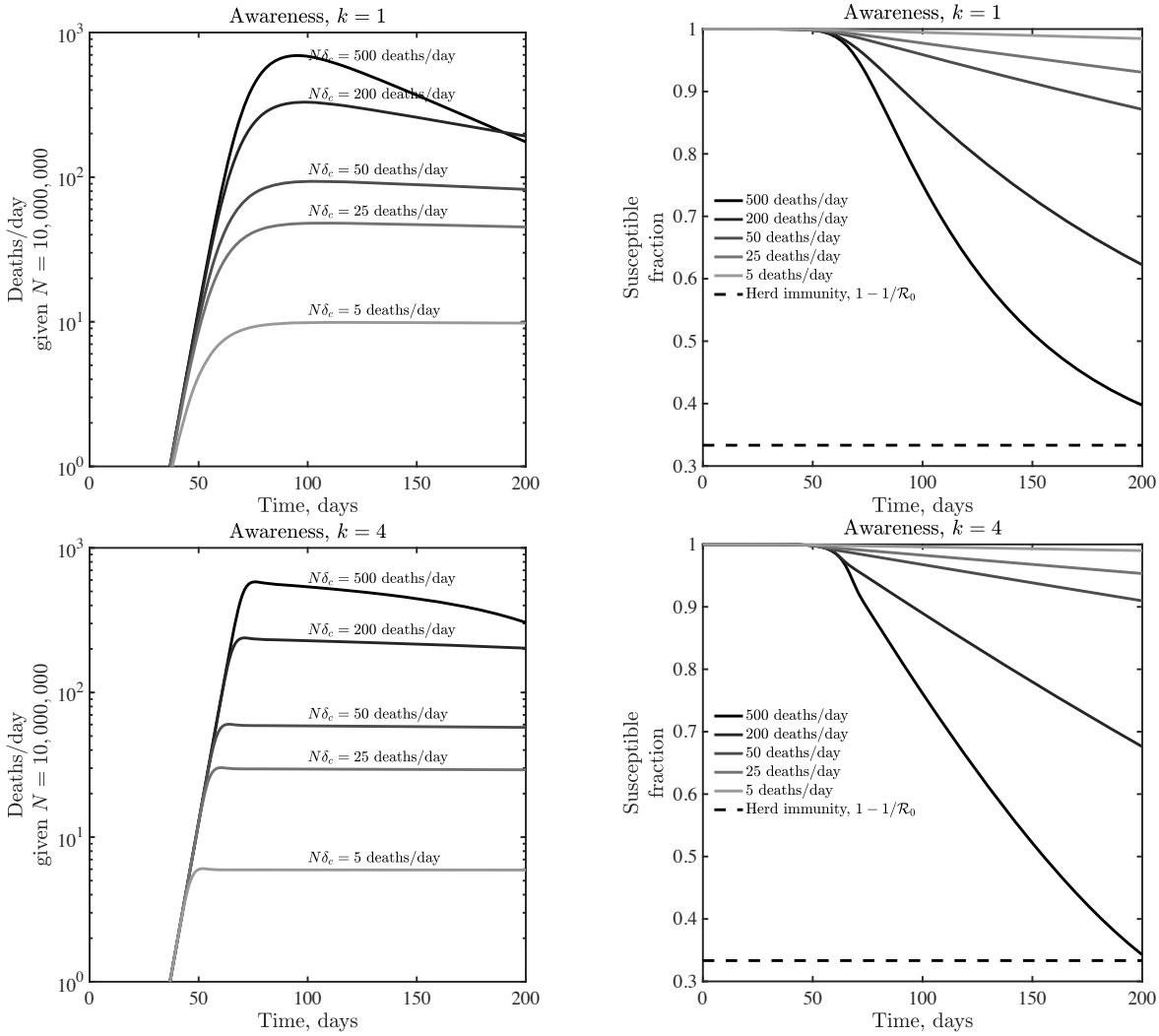

FIG. S1: Dynamics given variation in the critical fatality awareness level, δ_c for awareness $k = 1$ (top) and $k = 4$ (bottom). Panels show deaths/day (top) and the susceptible fraction as a function of time (bottom), the latter compared to a herd immunity level when only a fraction $1/\mathcal{R}_0$ remain susecptible. These simulations share the epidemiological parameters $\beta = 0.5$ /day, $\mu = 1/2$ /day, $\gamma = 1/6$ /day, and $f_D = 0.01$.

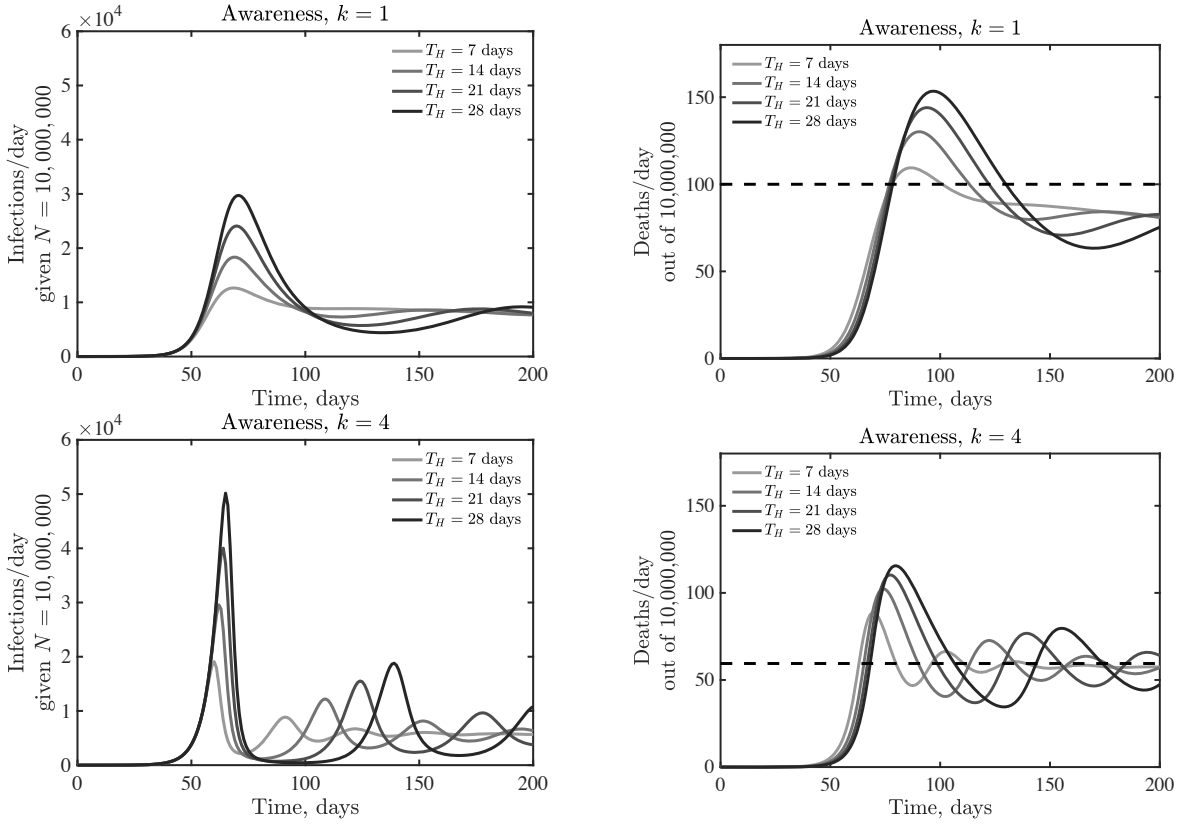

FIG. S2: Emergence of oscillatory dynamics in a death-driven awareness model of social distancing given lags between infection and fatality. Awareness is $k = 1$ (top) and $k = 4$ (bottom), all other parameters as in Figure 3. The dashed lines for fatalities expected quasi-stationary value $\delta^{(q)}$.